DOI: 10.1534/genetics.105.055210

Identification of Novel Mutations in *ACT1* and *SLA2* That Suppress the Actin-Cable-Overproducing Phenotype Caused by Overexpression of a Dominant Active Form of Bni1p in *Saccharomyces cerevisiae*

Shiro Yoshiuchi,*,† Takaharu Yamamoto,* Hiroshi Sakane,* Jun Kadota,* Junko Mochida,* Masahiro Asaka† and Kazuma Tanaka*,[1]

**Division of Molecular Interaction, Institute for Genetic Medicine and* †*Department of Gastroenterology and Hematology, Hokkaido University Graduate School of Medicine, Sapporo 060-0815, Japan*

Manuscript received January 3, 2006
Accepted for publication March 10, 2006

ABSTRACT

A formin Bni1p nucleates actin to assemble actin cables, which guide the polarized transport of secretory vesicles in budding yeast. We identified mutations that suppressed both the lethality and the excessive actin cable formation caused by overexpression of a truncated Bni1p (*BNI1ΔN*). Two recessive mutations, *act1-301* in the actin gene and *sla2-82* in a gene involved in cortical actin patch assembly, were identified. The isolation of *sla2-82* was unexpected, because cortical actin patches are required for the internalization step of endocytosis. Both *act1-301* and *sla2-82* exhibited synthetic growth defects with *bni1Δ*. *act1-301*, which resulted in an E117K substitution, interacted genetically with mutations in profilin (*PFY1*) and *BUD6*, suggesting that Act1-301p was not fully functional in formin-mediated polymerization. *sla2-82* also interacted genetically with genes involved in actin cable assembly. Some experiments, however, suggested that the effects of *sla2-82* were caused by depletion of actin monomers, because the temperature-sensitive growth phenotype of the *bni1Δ sla2-82* mutant was suppressed by increased expression of *ACT1*. The isolation of suppressors of the *BNI1ΔN* phenotype may provide a useful system for identification of actin amino-acid residues that are important for formin-mediated actin polymerization and mutations that affect the availability of actin monomers.

THE actin cytoskeleton plays essential roles in a diverse set of cellular processes, including cell polarization, cytokinesis, cell adhesions, and endocytosis. The dynamic organization of the actin cytoskeleton is spatially and temporally regulated. How the actin cytoskeleton assembles and functions, including how its assembly relates to its function, are fundamental questions in cell biology.

The budding yeast *Saccharomyces cerevisiae* is an excellent model system for studies of the actin cytoskeleton dynamics because yeast cells have a relatively simple actin cytoskeleton and offer powerful experimental tools. Throughout the yeast cell cycle, precisely choreographed changes in the organization of the actin cytoskeleton underlie spatial control of cell-surface growth and thereby determine cell morphology. Extension of the cell surface is preceded by the polarized organization of two actin-filament-containing structures: actin cables and cortical actin patches.

Actin cables, long bundles of actin filaments, are highly dynamic structures containing actin (Act1p), fimbrin (Sac6p), and tropomyosin (Tpm1p and Tpm2p). They originate from polarized sites such as a bud tip and extend throughout the mother cell along the cell axis. One major function of actin cables is to serve as tracks for the polarized transport of secretory vesicles by Myo2p, a type V myosin (Govindan *et al.* 1995; Pruyne *et al.* 1998). Bni1p and Bnr1p, members of the formin protein family, play an essential role in actin cable assembly (Evangelista *et al.* 2002; Sagot *et al.* 2002a) by stimulating actin nucleation (Pruyne *et al.* 2002; Sagot *et al.* 2002b). Formins are a family of highly conserved eukaryotic proteins implicated in a wide range of actin-based processes. These proteins are characterized by the presence of the juxtaposed formin homology (FH) domains, FH1 and FH2 (Evangelista *et al.* 2003). The proline-rich FH1 domain binds to the actin-monomer-binding protein profilin (Pfy1p), whereas the FH2 domain is sufficient for actin filament nucleation *in vitro*. Moreover, profilin–actin enhances nucleation by the FH1–FH2 domain but not the FH2 domain alone, suggesting that the interaction between the FH1 domain and profilin is required for increased nucleation (Pring *et al.* 2003). A 12S complex termed the polarisome comprises Bni1p, Spa2p, Pea2p, and Bud6p (Sheu *et al.* 1998), all of which are required for apical growth. In their absence, cells fail to confine a growth site to a small

[1]*Corresponding author:* Division of Molecular Interaction, Institute for Genetic Medicine, Hokkaido University Graduate School of Medicine, N-15 W-7, Kita-ku, Sapporo, Hokkaido 060-0815, Japan.
E-mail: k-tanaka@igm.hokudai.ac.jp

region during initial bud emergence and bud growth, resulting in a widened mother-bud neck and spherical, rather than ellipsoid, cell morphology (Sheu *et al.* 2000). Bud6p, like profilin, interacts with actin monomers and can enhance actin nucleation by Bni1p (Moseley *et al.* 2004).

Cortical actin patches and their associated proteins are involved in the internalization step of endocytosis (Engqvist-Goldstein and Drubin 2003). Cortical patches are associated with invaginations of the plasma membrane (Mulholland *et al.* 1994), have life times of only 5–20 sec (Smith *et al.* 2001), and are highly motile (Doyle and Botstein 1996; Waddle *et al.* 1996; Carlsson *et al.* 2002). The formation and reorganization of cortical actin patches are regulated by cortical-patch-like protein structures, including the Arp2/3 complex and several of its activators, and endocytic adaptors and scaffolds (Pruyne and Bretscher 2000). Sla2p, one of the patch components, contains an AP180 N-terminal homology (ANTH) domain that interacts with inositol phospholipids (Sun *et al.* 2005). In addition, Sla2p contains a central coiled-coil region and a talin homology domain at its C terminus (Yang *et al.* 1999). The talin homology domain binds to filamentous actin and is localized to actin structures when it alone is expressed *in vivo* (Yang *et al.* 1999). Real-time analyses of live *sla2*Δ mutant cells expressing enhanced green fluorescent protein-tagged patch assembly proteins revealed the formation of actin comet tail-like structures and inhibition of endocytic internalization, demonstrating that Sla2p negatively regulates assembly of actin filaments associated with endocytic vesicles (Kaksonen *et al.* 2003).

In this study, we found two new mutant alleles, *act1-301* and *sla2-82*, which suppressed growth defects caused by overexpression of an N-terminally truncated (dominant active) Bni1p. Both mutations suppressed the accumulation of the actin-cable-like structures induced by the truncated Bni1p. Our system provides a useful method to identify genes that affect the assembly or dynamics of actin cables.

MATERIALS AND METHODS

Strains, media, and genetic techniques: Yeast strains used in this study are listed in Table 1 with their genotypes. Strains were grown in rich YPDA medium [1% yeast extract (Difco Laboratories, Detroit), 2% bacto-peptone (Difco), 2% glucose, and 0.01% adenine] or YPGA medium (1% yeast extract, 2% bacto-peptone, 3% galactose, 0.2% sucrose, and 0.01% adenine). The lithium acetate method was used for introduction of plasmids into yeast cells (Elble 1992; Gietz and Woods 2002). Yeast strains carrying complete gene deletions (*bni1*Δ, *bud6*Δ, *end3*Δ, *mti1*Δ, and *vrp1*Δ); *GAL1* promoter-inducible *3HA-BNI1*Δ*1-1226*, *3HA-BNR1*Δ*1-755*, and *3HA-BNI1*; and green fluorescent protein (GFP)-tagged *MYO2* were constructed by PCR-based procedures as described (Longtine *et al.* 1998). The *pfy1-116* and *las17-11* mutants were constructed by three successive backcrosses into the YEF473 background strain. To construct YEF1159 (*sla2-*Δ*1* P_{GAL1}*-BNI1*Δ*N*), the P_{GAL1}*-BNI1* (*1227-1953*) fragment was integrated at the *LEU2* locus of YEF186 (*sla2-*Δ*1*). Strains carrying plasmids were selected in synthetic medium (SD) containing the required nutritional supplements. When indicated, synthetic galactose medium containing 0.5% casamino acids and 20 μg/ml tryptophan (SGA–Ura) was used. Standard genetic manipulations of yeast cells were performed as described previously (Sherman 2002).

Molecular biological techniques: PCR amplification was performed using a GeneAmp PCR System 9700 (Applied Biosystems, Foster City, CA). The DNA sequences of all constructs containing amplified PCR products were confirmed using an ABI PRISM BigDye Terminator Cycle sequencing ready reaction kit (Applied Biosystems) according to the manufacturer's protocol. DNA sequences were obtained using an ABI PRISM 310 DNA sequencer (Applied Biosystems). The plasmids used in this study are listed in Table 2. Schemes for the construction of plasmids and the sequences of PCR primers are available upon request. Two-hybrid analysis was performed using strain L40 containing the LexA–DNA-binding domain fusion plasmid and the Gal4-transcriptional activation domain fusion plasmid. The extent of the two-hybrid interaction was assayed by growth on SD–Trp–Leu–His plates.

Isolation of mutations that suppress the lethality caused by the overexpression of Bni1p(1227-1953): To isolate spontaneous mutants that overcome the growth inhibition caused by overexpression of the dominant active formin, YKT380 cells—in which *BNI1*Δ*1-1226*, the sole copy of *BNI1* in these cells, was expressed under the control of a galactose-inducible *GAL1* promoter (*HIS3::*P_{GAL1}*-3HA-BNI1*Δ*1-1226*)—were plated on 30 YPGA plates (1×10^7 cells/plate) and grown at 25° for 3 days. Eighty-seven revertants were picked up. To eliminate mutants in which the *GAL1* promoter was not induced, we transformed these mutants with pSMA111 (pRS316-P_{GAL10}-GIN11) or pRS316-P_{GAL7}-LacZ, which contained the *GIN11* gene that inhibits growth when overexpressed (Kawahata *et al.* 1999) and the *LacZ* gene under the control of galactose-inducible promoters, respectively. β-Galactosidase activity was measured by a 5-bromo-4-chloro-3-indolyl-β-D-galactopyranoside filter assay (Vojtek *et al.* 1993). Mutations in nine mutants were judged to specifically suppress the growth inhibition caused by Bni1p(1227-1953) overexpression. Tetrad analysis revealed that three of these nine clones carried a single recessive mutation that was responsible for the suppression. We found that the growth of two of these mutants was inhibited at 37° on glucose-containing medium. This temperature-sensitive growth phenotype cosegregated with the suppression of growth inhibition by Bni1p(1227-1953) overexpression and was suppressed by a single copy of *BNI1*. Another clone also showed a temperature-sensitive growth phenotype on glucose-containing medium, but this phenotype was not suppressed by a single copy of *BNI1*. To clone the mutated genes, we transformed the mutants with a YCp50–LEU2-based genomic library and isolated transformants that grew on glucose-containing plates at 37° but not on galactose-containing plate at 25°. Library plasmids were isolated, subcloning was performed by standard methods, and, using the linkage analysis, one allele each of *act1*, *pat1*, and *sla2* was isolated. During the course of cloning, we found that a plasmid harboring *ACT1* (YCp50–LEU2-2.4.1) suppressed the growth defect of the *bni1*Δ *sla2-82* mutant (see RESULTS).

Cloning of *act1-301* and *sla2-82*: To construct pRS316-ACT1, a *Bam*HI–*Eco*RI *ACT1* genomic fragment isolated from YCp–LEU2-2.4.1 was subcloned into the *Bam*HI–*Eco*RI gap of pRS316. pRS316-act1-301 was constructed by the gap-repair method using pRS316-ACT1 linearized with *Mun*I. To construct pRS313-SLA2gap, a 574-bp *Eco*RI–*Aat*II fragment and a 502-bp *Aat*II–*Sal*I fragment containing 5′- and 3′-flanking

TABLE 1

***S. cerevisiae* strains used in this study**

Strain[a]	Genotype	Reference or source
L40	*MAT***a** *lys2-801 his3Δ-200 trp1-901 leu2-3,112 ade2 LYS2::(lexAop)$_4$-HIS3 URA3::(lexAop)$_8$-lacZ*	Hollenberg *et al.* (1995)
DDY311	*MATα act1-2 his4-619 ura3-52*	Shortle *et al.* (1984)
DDY334	*MATα act1-4 ura3-52 ade2-101(am)*	Dunn and Shortle (1990)
DDY335	*MATα act1-3 tub2-201(benR) his3Δ200 leu2-3,112 ura3-52*	Shortle *et al.* (1984)
DDY338	*MAT***a** *act1-101::HIS3 tub2-201(benR) can1-1 cry1 ura3-52 leu2-3,112 his3Δ200*	Wertman *et al.* (1992)
DDY346	*MAT***a** *act1-119::HIS3 tub2-201(benR) cry1 ura3-52 leu2-3,112 his3Δ200 ade2-101(am)*	Wertman *et al.* (1992)
DDY347	*MAT***a** *act1-120::HIS3 tub2-201(benR) can1-1 cry1 ura3-52 leu2-3,112 his3Δ200*	Wertman *et al.* (1992)
DDY349	*MATα act1-124::HIS3 tub2-201(benR) ura3-52 leu2-3,112 his3Δ200*	Wertman *et al.* (1992)
DDY350	*MATα act1-125::HIS3 tub2-201(benR) ura3-52 leu2-3,112 his3Δ200*	Wertman *et al.* (1992)
DDY1024	*MAT***a** *pfy1-116::LEU2 his3Δ-200 leu2-3,112 lys2-801 ura3-52 ade3 ade2-101*	Gift from D. Drubin
DDY1492	*MATα act1-159::HIS3 tub2-201(benR) leu2-3,112 ura3-52 ade2? ade4*	Belmont and Drubin (1998)
DDY1960	*MAT***a** *las17-11::LEU2 his3Δ-200 leu2-3,112 lys2-801 ura3-52 ade2-101*	Gift from D. Drubin
YEF473	*MAT***a**/α *ura3-52/ura3-52 his3Δ-200/his3Δ-200 trp1Δ-63/trp1Δ-63 leu2Δ-1/leu2Δ-1 lys2-801/lys2-801*	Longtine *et al.* (1998)
YKT38[a]	*MAT***a** *ura3-52 his3Δ-200 trp1Δ-63 leu2Δ-1 lys2-801*	Mochida *et al.* (2002)
YKT380	*MAT***a** *HIS3::P$_{GAL1}$-3HA-BNI1Δ1-1226(P$_{GAL1}$-BNI1ΔN)*	This study
YKT967	*MAT***a** *HIS3::P$_{GAL1}$-BNI1ΔN act1-301*	This study
YKT846	*MATα HIS3::P$_{GAL1}$-BNI1ΔN sla2-82*	This study
YKT542	*MATα HIS3::P$_{GAL1}$-3HA-BNR1Δ1-755(P$_{GAL1}$-BNR1ΔN)*	This study
YKT991	*MAT***a** *HIS3::P$_{GAL1}$-BNR1ΔN act1-301*	This study
YKT992	*MAT***a** *HIS3::P$_{GAL1}$-BNR1ΔN sla2-82*	This study
YKT379	*MAT***a**/α *HIS3::P$_{GAL1}$-BNI1ΔN/BNI1*	This study
YKT1091	*MAT***a**/α *HIS3::P$_{GAL1}$-BNI1ΔN/BNI1 act1-301::HphMX4/act1-301::HphMX4*	This study
YKT1092	*MAT***a**/α *HIS3::P$_{GAL1}$-BNI1ΔN/BNI1 sla2-82/sla2-82*	This study
YKT986	*MAT***a** *act1-301*	This study
YKT847	*MAT***a** *sla2-82*	This study
YKT446	*MAT***a** *bni1Δ::HphMX4*	This study
YKT968	*MAT***a** *bni1Δ::HphMX4 act1-301*	This study
YKT853	*MAT***a** *bni1Δ::HIS3MX6 sla2-82*	This study
YKT662	*MAT***a** *MYO2-GFP::TRP1*	This study
YKT1058	*MAT***a** *act1-301::HphMX4 MYO2-GFP::TRP1*	This study
YKT1057	*MAT***a** *bni1-116 MYO2-GFP::TRP1*	This study
YKT1060	*MAT***a** *act1-301::HphMX4 bni1-116 MYO2-GFP::TRP1*	This study
YKT977	*MAT***a** *pfy1-116::LEU2*	This study
YKT988	*MAT***a** *act1-301 pfy1-116::LEU2*	This study
YKT616	*MAT***a** *bud6Δ::kanMX6*	This study
YKT990	*MAT***a** *act1-301 bud6Δ::kanMX6*	This study
YKT1089	*MAT***a** *sla2-82::KanMX6 bud6Δ::HIS3*	This study
YKT1090	*MAT***a** *sla2-82::KanMX6 pfy1-116::LEU2*	This study
YKT1059	*MAT***a** *sla2-82::KanMX6 MYO2-GFP::TRP1*	This study
YKT1061	*MAT***a** *sla2-82::KanMX6 bni1-116 MYO2-GFP::TRP1*	This study
YKT979	*MATα HIS3::P$_{GAL1}$-BNI1ΔN arp2-2::URA3*	This study
YKT980	*MATα HIS3::P$_{GAL1}$-BNI1ΔN end3Δ::HphMX4*	This study
YKT981	*MATα HIS3::P$_{GAL1}$-BNI1ΔN las17-11::LEU2*	This study
YKT414	*MAT***a** *HIS3::P$_{GAL1}$-3HA-BNI1*	This study
YKT984	*MAT***a** *HIS3::P$_{GAL1}$-3HA-BNI1 mti1Δ::KanMX6*	This study
YKT189	*MAT***a** *mti1Δ::KanMX6*	This study
YKT680	*MAT***a** *vrp1Δ::KanMX6*	This study
YKT982	*MAT***a** *bni1Δ::HphMX4 vrp1Δ::KanMX6*	This study
YKT983	*MAT***a** *mti1Δ::HIS3MX6 vrp1Δ::KanMX6*	This study
YKT859	*MAT***a** *sla2Δ502-968-3HA::TRP1*	This study
YKT861	*MAT***a** *sla2Δ768-968-3HA::TRP1*	This study
YKT186	*MAT***a** *sla2-Δ1::URA3*	This study
YKT1159	*MAT***a** *sla2-Δ1::URA3 LEU2:: P$_{GAL1}$-BNI1ΔN*	This study

[a] YKT strains are isogenic derivatives of YEF473.

TABLE 2

Plasmids used in this study

Plasmid	Characteristic	Source
pSMA111	*P_{GAL10}-GIN11 URA3 CEN6*	Kawahata *et al.* (1999)
pRS316-P_{GAL7}-LacZ	*P_{GAL7}-LacZ URA3 CEN6*	This study
pRS314	*TRP1 CEN6*	Sikorski and Hieter (1989)
pRS314-BNI1 (pKY1226)	*BNI1 TRP1 CEN6*	Kadota *et al.* (2004)
pRS314-bni1-116 (pKT1426)	*bni1-116 TRP1 CEN6*	This study
pRS314-bni1(D1511G) (pKT1427)	*bni1(D1511G) TRP1 CEN6*	This study
pRS314-bni1-FH2#1 (pKT1428)	*bni1-FH2#1 TRP1 CEN6*	This study
pRS314-BNI1(Δ6-642) (pKT1419)	*BNI1(Δ6-642) TRP1 CEN6*	This study
pRS314-BNI1(Δ826-986) (pKT1421)	*BNI1(Δ826-986) TRP1 CEN6*	Kadota *et al.* (2004)
pRS314-BNI1(1−1750) (pKT1422)	*BNI1(1−1750) TRP1 CEN6*	Kadota *et al.* (2004)
pRS314-BNI1(Δ1228-1414) (pKT1423)	*BNI1(Δ1228-1414) TRP1 CEN6*	Kadota *et al.* (2004)
pRS314-BNI1(Δ1553-1646) (pKT1424)	*BNI1(Δ1553-1646) TRP1 CEN6*	Kadota *et al.* (2004)
pRS316-P_{GAL1}-HA	*P_{GAL1}-HA URA3 CEN6*	Kamei *et al.* (1998)
pRS316-P_{GAL1}-HA-BNI1(1227-1953) (pKT1605)	*P_{GAL1}-HA-BNI1(1227-1953) URA3 CEN6*	This study
pBTM116-HA	DBD_{LexA}[a]-HA *TRP1* 2 μm	Imamura *et al.* (1997)
pBTM116-HA-PFY1	DBD_{LexA}-HA-PFY1 *TRP1* 2 μm	Gift from Y. Takai
pBTM116-HA-BUD6(221-788) (pKT1571)	DBD_{LexA}-HA-BUD6(221-788) *TRP1* 2 μm	This study
pBTM116-HA-BNI1(1227-1953) (pKT1572)	DBD_{LexA}-HA- BNI1(1227-1953) *TRP1* 2 μm	This study
pBTM116-HA-BNI1(1227-1750) (pKT1573)	DBD_{LexA}-HA-BNI1(1227-1750) *TRP1* 2 μm	This study
pACTII-HK	AD_{GAL4}[a] *LEU2* 2 μm	Ozaki *et al.* (1996)
pACTII-HK-ACT1 (pKT1574)	AD_{GAL4}-ACT1 *LEU2* 2 μm	This study
pACTII-HK-ACT1-301 (pKT1575)	AD_{GAL4}-act1-301 *LEU2* 2 μm	This study
pRS313-sla2Δ33-359 (pDD367)	*sla2Δ33-359 HIS3 CEN6*	Yang *et al.* (1999)
pRS313-sla2Δ33-501 (pDD364)	*sla2Δ33-501 HIS3 CEN6*	Yang *et al.* (1999)
pRS313-sla2Δ33-750 (pDD362)	*sla2Δ33-750 HIS3 CEN6*	Yang *et al.* (1999)
pRS313-sla2Δ360-575 (pDD371)	*sla2Δ360-575 HIS3 CEN6*	Yang *et al.* (1999)
pRS316	*URA3 TRP1*	Sikorski and Hieter (1989)
pRS316-ACT1 (pKT1412)	*ACT1 URA3 CEN6*	This study
pRS316-ACT1-301 (pKT1576)	*act1-301 URA3 CEN6*	This study
pRS316-BNI1 (pKT1227)	*BNI1 URA3 CEN6*	Kadota *et al.* (2004)
pRS305	*LEU2*	Sikorski and Hieter (1989)
pRS305-P_{GAL1}-HA-BNI1(1227-1953) (pKT1606)	*P_{GAL1}-HA-BNI1(1227-1953) LEU2*	This study

[a] DBD_{LexA} and AD_{GAL4} are the DNA-binding domain of LexA and the transcriptional activating domain of Gal4p, respectively.

regions of the *SLA2* gene, respectively, were amplified by PCR and cloned into the *Eco*RI–*Sal*I gap of pRS313. *SLA2* and *sla2-82* were cloned by the gap-repair method using pRS313-SLA2gap linearized with *Aat*II.

Microscopic observations: Cells expressing Myo2p–GFP were fixed for 10 min by the direct addition of 37% formaldehyde stock solution (Wako Pure Chemical Industries, Osaka, Japan) to a 3.7% final concentration in medium and observed using a GFP bandpass filter set (excitation, 460–500 nm; dichroic mirror, 505 nm; emission, 510–560 nm). To visualize the actin cytoskeleton, cells were fixed as described above, harvested, and fixed again for 1 hr in phosphate-buffered saline (PBS) containing 3.7% formaldehyde. Fixed cells were incubated for 30 min at room temperature in 1 μM tetramethylrhodamine isothiocyanate (TRITC)-phalloidin (Sigma Chemical, St. Louis). Following three washes with PBS, cells were mounted in 50% glycerol containing *n*-propyl gallate (Wako). Cells were observed using a G-2A TRITC filter set (excitation, 510–560 nm; dichroic mirror, 575 nm; emission, 590 nm). Microscopic observation was performed as described previously (Mochida *et al.* 2002). To quantify the polarized localization of Myo2p–GFP, at least 200 small-budded cells were randomly selected and observed. Small buds were identified to be <30% the size of the mother cell.

RESULTS

Identification of *act1-301* and *sla2-82* mutations that suppress the growth inhibition caused by overexpression of a dominant active Bni1p: Overexpression of NH_2-terminally truncated forms of Bni1p or Bnr1p leads to disorganization of the actin cytoskeleton, including the production of an excessive number of actin cables and the depolarization of actin patches, resulting in inhibition of cell growth (Evangelista *et al.* 1997; Kikyo *et al.* 1999). To search for regulators of actin cytoskeletal reorganization, we screened for mutations that suppressed the growth inhibition caused by overexpression of NH_2-terminally truncated Bni1p. *P_{GAL1}-3HA-BNI1Δ1-1226* (*P_{GAL1}-BNI1ΔN*) mutant cells overexpress a truncated Bni1p, Bni1p(1227-1953), which contains the FH1 and FH2 domains. This mutant does not grow in galactose medium, in which the *GAL1* promoter is induced. We screened for spontaneous revertants that could grow in galactose medium. We isolated three independent revertants that each carried a single recessive

mutation and cloned the affected genes. The first gene, *ACT1*, is the only gene that encodes actin in budding yeast. The second gene, *PAT1*, is involved in mRNA decapping (Bonnerot *et al.* 2000). The third gene, *SLA2*, codes for Sla2p, a protein involved in the assembly of cortical actin patches (Holtzman *et al.* 1993; Raths *et al.* 1993). We next investigated how the *act1* and *sla2* mutant alleles (designated *act1-301* and *sla2-82*, respectively) suppressed the phenotypes caused by overexpression of a truncated Bni1p. Both *act1-301* and *sla2-82* also suppressed the growth defect of *BNR1*Δ*N*-overexpressing cells as well as that of the *BNI1*Δ*N*-overexpressing cells (Figure 1A). P_{GAL1}-*BNI1*Δ*N* cells carrying *act1-301* or *sla2-82* showed normal spherical morphology and polarized distributions of cortical actin patches and actin cables (Figure 1B), indicating that these mutations suppressed the excessive formation of actin cables. Interestingly, both *act1-301* and *sla2-82* showed synthetic growth defects with *bni1*Δ at higher temperatures (Figures 1C, 3A, and 5B).

Act1-301p seems to impair Bni1p-catalyzed actin polymerization: We cloned the *act1-301* mutant gene and determined its DNA sequence. *act1-301* contained a point mutation resulting in the substitution of a Lys residue for a Glu residue at amino-acid position 117. For *act1-301* mutant cells, the growth rates at low and high temperatures, cell morphology, polarized distributions of actin patches and cables, and fluid-phase endocytosis as assayed by the uptake of Lucifer yellow were indistinguishable from wild-type cells (data not shown), indicating that the E117K substitution did not severely impair the functions of Act1-301p.

The FH2 domain of Bni1p is required for actin cable assembly *in vivo* (Evangelista *et al.* 2002; Sagot *et al.* 2002a) and stimulates actin polymerization *in vitro* (Pruyne *et al.* 2002; Sagot *et al.* 2002b). In the absence of *BNR1*, a structural and functional homolog of *BNI1* with a minor role, three temperature-sensitive alleles of *BNI1* that produce proteins with amino-acid substitutions in the FH2 domain—*bni1-116* (V1475A, K1498E, and D1511N) (Kadota *et al.* 2004), *bni1-11* (D1511G and K1601R) (Evangelista *et al.* 2002; Pruyne *et al.* 2002), and *bni1-FH2#1* (R1528A and R1530A)—cause actin cables to rapidly disappear when the mutant cells are incubated at high temperatures. The Bni1FH2#1 protein also exhibits defective actin polymerization *in vitro* (Sagot *et al.* 2002b). We found that the phenotype caused by *bni1-11* was the result of a single amino-acid substitution, D1511G (data not shown). Similar to *bni1*Δ, the *bni1* alleles *bni1-116*, *bni1(D1511G)*, and *bni1-FH2#1*, when combined with *act1-301*, caused the temperature-sensitive growth phenotypes (Figure 2A). These results suggest that the actin-polymerizing activity of Bni1p is relevant to the genetic interaction of *bni1* mutations with *act1-301*.

The temperature-sensitive growth of *bni1*Δ *act1-301* mutant cells seems to be due to defective actin cable

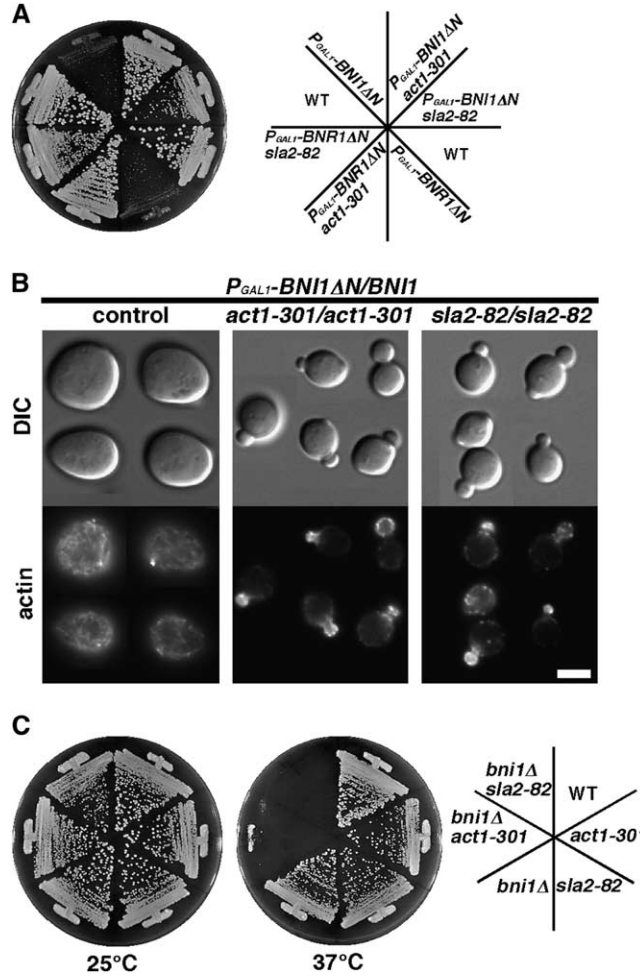

Figure 1.—Identification of *act1-301* and *sla2-82*. (A) *act1-301* and *sla2-82* mutations suppress growth defects caused by overexpression of a dominant active *BNI1* or *BNR1*. Strains grown on a YPDA plate were streaked onto a YPGA plate, followed by incubation at 30° for 3 days. WT (wild-type strain), YKT38; P_{GAL1}-*BNI1*Δ*N*, YKT380; P_{GAL1}-*BNI1*Δ*N act1-301*, YKT967; P_{GAL1}-*BNI1*Δ*N sla2-82*, YKT846; P_{GAL1}-*BNR1*Δ*N*, YKT542; P_{GAL1}-*BNR1*Δ*N act1-301*, YKT991; P_{GAL1}-*BNR1*Δ*N sla2-82*, YKT992. (B) *act1-301* and *sla2-82* suppress the morphological and actin cytoskeletal defects caused by overexpression of a dominant active *BNI1*. Strains grown in YPDA were shifted to YPGA medium and cultured at 30° for 12 hr. Cells were fixed, labeled with TRITC–phalloidin, and visualized by differential interference contrast or with a TRITC filter. P_{GAL1}-*BNI1*Δ*N/BNI1* (control), YKT379; P_{GAL1}-*BNI1*Δ*N/BNI1 act1-301/act1-301*, YKT1091; P_{GAL1}-*BNI1*Δ*N/BNI1 sla2-82/sla2-82*, YKT1092. Bar, 5 μm. (C) Both *act1-301* and *sla2-82* show synthetic growth defects with *bni1*Δ. Strains were streaked onto YPDA plates, followed by incubation at 25° for 3 days or at 37° for 2 days. WT, YKT38; *act1-301*, YKT986; *sla2-82*, YKT847; *bni1*Δ, YKT446; *bni1*Δ *act1-301*, YKT968; *bni1*Δ *sla2-82*, YKT853.

formation. Labeling of actin cables with phalloidin, however, did not allow us to examine this possibility, because almost no actin cables could be detected in the *bni1*Δ cells (data not shown). Therefore, we visualized a GFP-tagged type V myosin, Myo2p–GFP, whose polarized localization depends on actin cables (Karpova *et al.*

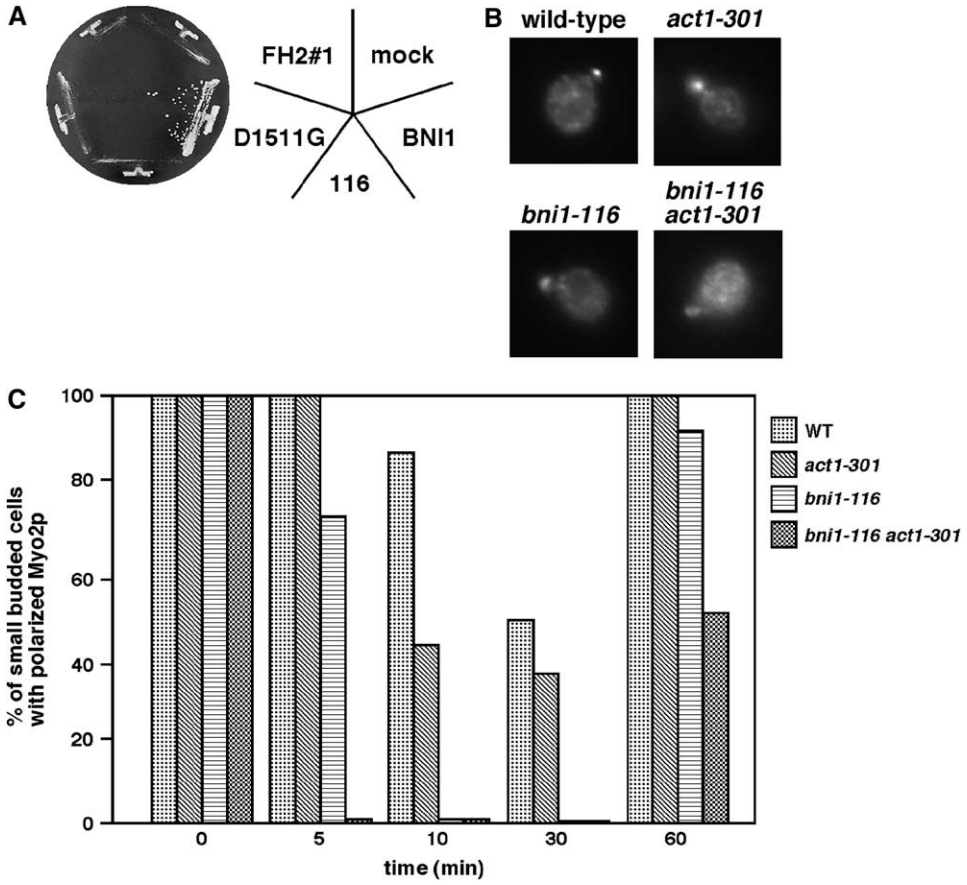

FIGURE 2.—Defects caused by *act1-301* are tied to Bni1p-mediated actin polymerization. (A) *act1-301* shows synthetic growth defects with mutations in the FH2 domain of Bni1p. The *bni1*Δ *act1-301* strain (YKT968) was transformed with pRS314 (mock), pRS314-BNI1 (BNI1), pRS314-bni1-116 (116), pRS314-bni1(D1511G) (D1511G), or pRS314-bni1-FH2#1 (FH2#1). The transformants were streaked onto a YPDA plate, followed by incubation at 37° for 2 days. (B) Mislocalization of Myo2p–GFP in *bni1 act1-301* mutant. YKT662 (*MYO2–GFP*), YKT1058 (*act1-301 MYO2–GFP*), YKT1057 (*bni1-116 MYO2–GFP*, wild-type), and YKT1060 (*bni1-116 act1-301 MYO2–GFP*) were grown in YPDA medium at 25° and then shifted to 37° for 5 min. Cells were fixed and observed by fluorescence microscopy. (C) A time course of the polarized localization of Myo2p–GFP in small-budded cells. The strains described in B were grown in YPDA medium at 25° and then shifted to 37° for the indicated periods of time. Cells were fixed and at least 200 small-budded cells were observed for each data point by fluorescence microscopy.

2000) in *bni1-116 act1-301* mutant cells. Because a fraction of Myo2p–GFP is localized at bud tips in an actin-independent manner (AYSCOUGH *et al.* 1997), we examined the time course of polarized Myo2p–GFP localization after a temperature upshift. *act1-301* alone did not affect Myo2p–GFP localization after a 5-min incubation at 37°, but, after 10 and 30 min, slightly enhanced the mislocalization of Myo2p that was seen in wild-type cells. In the *bni1-116* single mutant, Myo2p–GFP was slightly mislocalized after a 5-min incubation at 37° and completely mislocalized after 30 min. Myo2p–GFP was completely mislocalized even after a 5-min incubation at 37° in the *bni1-116 act1-301* mutant (Figure 2, B and C). These results suggest that *act1-301* exacerbates the actin-cable-assembly defects in the *bni1-116* mutant.

***act1-301* genetically interacts with a mutation in profilin and *BUD6*:** The genetic interactions between *act1-301* and other genes related to Bni1p function were further investigated. *act1-301* showed synthetic growth defects with the mutant profilin allele *pfy1-116* and *bud6*Δ, but not with *spa2*Δ (Figure 3A). Interestingly, the synthetic growth defect with *bud6*Δ was more severe: the *bud6*Δ *bni1-116 act1-301* mutant did not grow even at 30°. Pfy1p and Bud6p interact with the FH1 and the COOH-terminal domains of Bni1p, respectively (EVANGELISTA *et al.* 1997). These proteins specifically bind actin monomers to stimulate nucleotide exchange (MOSELEY *et al.* 2004). We examined whether the interactions of Bni1p with these proteins are required for *act1-301* mutant cells to grow. Truncation mutants of Bni1p, which lacked the domains that interact with Rho/Cdc42p (ΔRBD), Spa2p (ΔSBD), Pfy1p (ΔFH1), or Bud6p (ΔBBD), or lacked the FH2 domain (ΔFH2), were expressed in *bni1*Δ *act1-301* mutant cells and cell growth at 37° was examined (Figure 3B). Proper expression of the mutant proteins was confirmed by immunoblotting for *myc*-tagged versions of the truncated Bni1ps (data not shown). ΔSBD fully restored growth, whereas ΔRBD only weakly restored it. ΔFH1, ΔFH2, and ΔBBD, however, failed to restore any growth. Our results suggest that *act1-301* affected the assembly of actin cables, a process in which Bni1p acts to polymerize actin through interactions with Pfy1p and Bud6p. We examined the physical interaction between Act1-301p and Pfy1p or Bud6p by the two-hybrid method. Act1-301p, however, interacted with both Pfy1p and Bud6p to an extent similar to that of Act1p (Figure 3C). Furthermore, when we examined the interaction between Act1-301p and Bni1p fragments containing the FH1 and FH2 domains, we found that Act1-301p and Act1p interacted with Bni1p(1227-1953) to a similar extent. Bni1p(1227-1750), which lacked the Bud6p-binding domain, also interacted with both Act1-301p and Act1p (Figure 3C), but

A

strain	30°C	35°C	37°C
wild-type	+++	+++	+++
act1-301	+++	+++	+++
pfy1-116	+++	+++	++
pfy1-116 act1-301	+++	+++	±
bud6Δ	+++	+++	+++
bud6Δ act1-301	+	−	−
bni1-116	+++	+++	++
bni1-116 act1-301	+++	++	±
bud6Δ bni1-116 act1-301	−	ND	ND
spa2Δ	+++	+++	+++
spa2Δ act1-301	+++	+++	+++

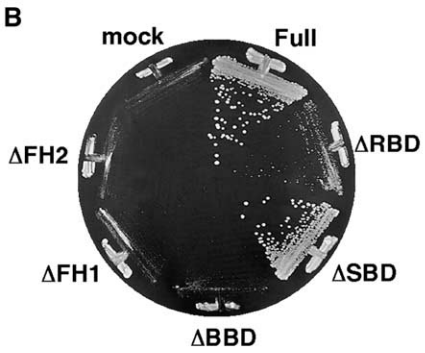

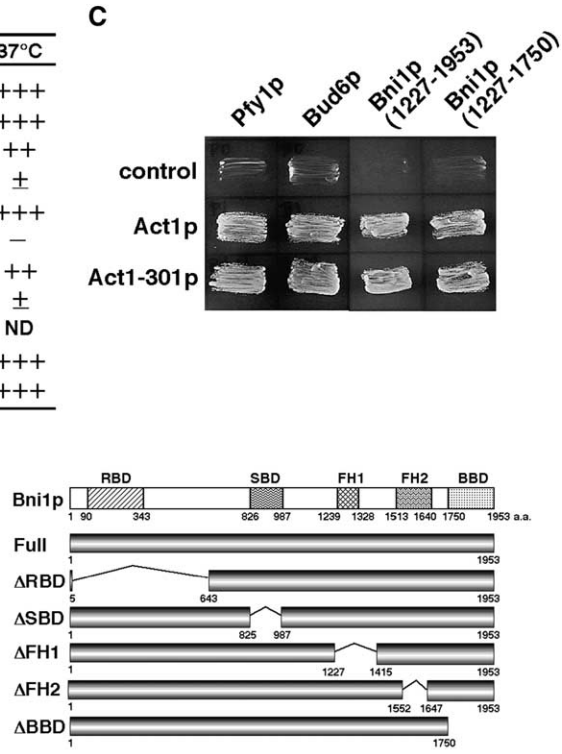

FIGURE 3.—The profilin- and Bud6p-related functions of Act1-301p are defective. (A) *act1-301* shows synthetic growth defects with *bud6* and *pfy1-116*. Strains were streaked onto YPDA plates, followed by incubation at the indicated temperatures for 2 days. Symbols indicate relative growth rates from wild type (+++) to no growth (−). (B) The interaction of Bni1p with Pfy1p or Bud6p, but not with Rho/Cdc42p or Spa2p, is required for Bni1p to alleviate the *act1-301* phenotypes. (Right) The structures of the truncated Bni1p proteins. The numbers indicate the positions of the amino-acid residues. The represented domains are the Rho-binding domain (RBD), the Spa2p-binding domain (SBD), formin homology domains (FH1 and FH2), and the Bud6p-binding domain (BBD). The *bni1Δ act1-301* strain (YKT968) was transformed with pRS314 (mock), pRS314-BNI1 (Full), pRS314-bni1Δ6-642 (ΔRBD), pRS314-bni1Δ826–986 (ΔSBD), pRS314-bni1(1–1750) (ΔBBD), pRS314-bni1Δ1228–1414 (ΔFH1), or pRS314-bni1Δ1553–1646 (ΔFH2). The transformants were streaked onto a YPDA plate, followed by incubation at 37° for 2 days. (C) Act1-301p interacts with Pfy1p, Bud6p, Bni1p(1227–1953), and Bni1p(1227–1750) in the two-hybrid method. DNA fragments encoding *ACT1* or *act1-301* were cloned into the pACTII vector (Gal4-transcriptional activation domain vector) and the resultant plasmids were introduced into an L40 cell expressing Pfy1p, Bud6p, Bni1p(1227–1953), or Bni1p(1227–1750) fused with LexA–DNA-binding domain. Each transformant was patched onto an SD plate without histidine, followed by incubation at 30° for 2 days. Protein interactions were examined qualitatively by histidine auxotrophy.

Bni1p(1348-1953), which lacked the FH1 domain, did not (data not shown). Since Pfy1p binds to the FH1 domain, the two-hybrid interaction of Bni1p with actin may be mediated by the interaction between Bni1p and Pfy1p.

The previously isolated *act1-101* mutation also acts as a suppressor of the growth defects caused by the *BNI1ΔN* overexpression: Our identification of *act1-301* suggests that isolation of suppressor mutations of the *BNI1ΔN*-overexpressing mutant is useful to identify amino-acid residues that are specifically required for the actin cable assembly. Previously, a large collection of *act1* mutant alleles, which affect residues over the surface of Act1p protein, was generated by alanine-scanning mutagenesis (WERTMAN *et al.* 1992). We examined five of these alleles and four other temperature-sensitive *act1* mutant alleles for the suppression of growth defects of the *BNI1ΔN*-overexpressing cells. Interestingly, *act1-101* (D363A, E364A) displayed the suppression (Figure 4). Aspartate 363 and glutamate 364 of Act1p also may be involved in the formin-mediated actin polymerization.

***sla2-82* genetically interacts with mutations in other actin-cable-related genes:** Phenotypic suppression of P_{GAL1}-*BNI1ΔN* by *sla2-82* and the synthetic growth defect between *bni1Δ* and *sla2-82* are surprising, because Sla2p is a component of the machinery that assembles cortical actin patches. When *sla2-82* was combined with *bni1-116*, *bni1(D1511G)*, or *bni1-FH2#1*, the resulting double mutants showed a temperature-sensitive growth phenotype (Figure 5A), indicating that the actin-polymerizing activity of Bni1p is relevant to the genetic interaction of *bni1* mutations with *sla2-82*. We further examined the genetic interactions of *sla2-82* with mutations in actin-cable-related genes and found that *sla2-82* exhibited synthetic growth defects with both *pfy1-116* and *bud6Δ* (Figure 5B). Experiments using the *BNI1* deletion constructs schematized in Figure 3B also suggested that the interaction of Bni1p with Pfy1p and Bud6p was required for *sla2-82* mutant cells to grow (Figure 5C). Defective assembly of actin cables in the *bni1Δ sla2-82* mutant was further examined by the observation of Myo2p–GFP. *sla2-82* alone slightly enhanced Myo2p–GFP mislocalization in wild-type cells after incubations of 5–30 min at 37°. In contrast, Myo2p–GFP was completely mislocalized even after a 5-min incubation at 37° in the *bni1-116 sla2-82* mutant (Figure 6, A and B). These results suggest that *sla2-82* exacerbates the defects

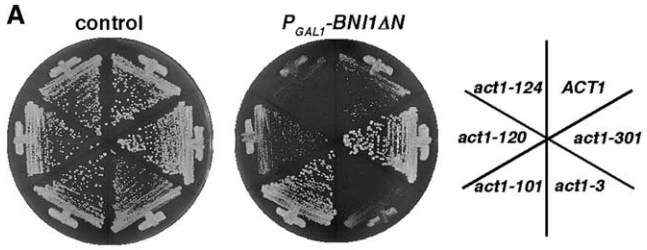

B

suppress
act1-301 (E117K), *act1-101* (D363A, E364A)
not suppress
act1-2 (A58T), *act1-3* (P32L), *act1-4* (E259V), *act1-119* (R116A, E117A, K118A), *act1-120* (E99A, E100A), *act1-124* (D56A, E57A), *act1-125* (K50A, D51A), *act1-159* (V159N)

FIGURE 4.—Effect of various *act1* alleles on the growth defect caused by overexpression of a dominant active *BNI1*. *act1* strains were transformed with pRS316-P_{GAL1}-HA (control) or pRS316-P_{GAL1}-HA-BNI1ΔN (P_{GAL1}-*BNI1ΔN*). The transformants were streaked onto an SGA–Ura plate, followed by incubation at 30° for 2 days. Representative results were shown in A and the results were summarized in B. Strains used were as follows: *ACT1*, YKT38; *act1-301*, YKT986; *act1-3*, DDY335; *act1-101*, DDY338; *act1-120*, DDY347; *act1-124*, DDY349; *act1-2*, DDY311; *act1-4*, DDY334; *act1-119*, DDY346; *act1-125*, DDY377; *act1-159*, DDY1492.

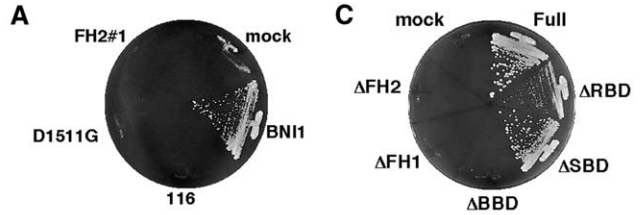

B

strain	25°C	30°C	35°C	37°C
wild-type	+++	+++	+++	+++
sla2-82	+++	+++	+++	+++
bni1Δ	+++	+++	+++	+++
bni1Δ sla2-82	++	++	+	±
pfy1-116	+++	+++	+++	++
pfy1-116 sla2-82	+++	+++	+	−
bud6Δ	+++	+++	+++	+++
bud6Δ sla2-82	+	±	−	−
spa2Δ	+++	+++	+++	+++
spa2Δ sla2-82	+++	+++	+++	+++

FIGURE 5.—*sla2-82* interacts with mutations in actin-cable-related genes. (A) *sla2-82* shows synthetic growth defects with mutations in the FH2 domain of Bni1p. The *bni1Δ sla2-82* strain (YKT853) was transformed with pRS314 (mock), pRS314-BNI1 (BNI1), pRS314-bni1-116 (116), pRS314-bni1(D1511G) (D1511G), or pRS314-bni1-FH2#1 (FH2#1). The transformants were streaked onto a YPDA plate, followed by incubation at 37° for 2 days. (B) *sla2-82* shows synthetic growth defects with *bud6* and *pfy1-116*. Strains were streaked onto YPDA plates, followed by incubation at the indicated temperature for 2 days. Symbols indicate relative growth rates from wild-type (+++) to no growth (−). (C) Interaction of Bni1p with Pfy1p or Bud6p, but not with Rho/Cdc42p or Spa2p, is required for Bni1p to suppress the *sla2-82* deficiencies. The *bni1Δ sla2-82* strain (YKT853) was transformed with plasmids described in Figure 3B. The transformants were streaked onto a YPDA plate, followed by incubation at 37° for 2 days.

in cells carrying mutations in genes related to actin cable assembly.

Synthetic growth defects of the *bni1Δ sla2-82* mutant may be due to depletion of the actin monomer pool: Phenotypic suppression of P_{GAL1}-*BNI1ΔN* by mutations in other components involved in actin patch assembly was examined. *arp2-1*, *end3Δ*, and *las17-11*, however, failed to suppress the growth defect of the P_{GAL1}-*BNI1ΔN* mutant (Figure 7A). Moreover, synthetic growth defects with *bni1Δ* were not observed for *sla1Δ*, *abp1Δ*, *arp2-1*, and *las17Δ* (Figure 7B), suggesting that the genetic interaction with actin-cable-related mutations was specific to *sla2-82*.

The functional difference between Sla2p and the actin patch proteins examined above is that Sla2p negatively regulates the assembly of actin patches (KAKSONEN *et al.* 2003). In the *sla2Δ* mutant, actin is continuously nucleated from nonmotile endocytic complexes, resulting in the formation of actin comet tail-like structures. We reasoned that the *sla2-82* mutation also caused the sequestration of actin monomers in the actin comet tails, which might render the impaired actin-cable-assembly machinery incapable of assembling a sufficient number of actin cables to allow polarized growth. Consistent with this hypothesis, increasing the number of copies of *ACT1* suppressed the growth defect of the *bni1Δ sla2-82* mutant and partially suppressed the Myo2p–GFP mislocalization in the *bni1-116 sla2-82* mutant (Figure 8, A and B). Mti1p/Bbc1p, another negative regulator of actin patch assembly, inhibits Las17p from activating the Arp2/3 complex (RODAL *et al.* 2003). *mti1Δ* also exhibited a synthetic growth defect with *bni1Δ* (Figure 8C; TONG *et al.* 2001). We previously showed that *mti1Δ* suppressed the temperature-sensitive growth phenotype observed in cells carrying a mutation in *VRP1*, a positive regulator of actin patch assembly (MOCHIDA *et al.* 2002). If genetic interactions between genes related to actin cables and actin patches occur depending on the availability of monomeric actin, *bni1Δ* may have suppressed *vrp1Δ*, because the size of the actin pool available for actin patch assembly would be increased in the *bni1Δ* mutant. The temperature-sensitive growth phenotype of *vrp1Δ* mutants was suppressed by *bni1Δ* as well as by *mti1Δ* (Figure 8D).

Deletion analysis of *SLA2* for the suppression of growth defects of the *BNI1ΔN*-overexpressing cells: Several structural motifs and functional domains have been identified in Sla2p (YANG *et al.* 1999; SUN *et al.* 2005) (Figure 9). The NH_2-terminal ANTH domain of

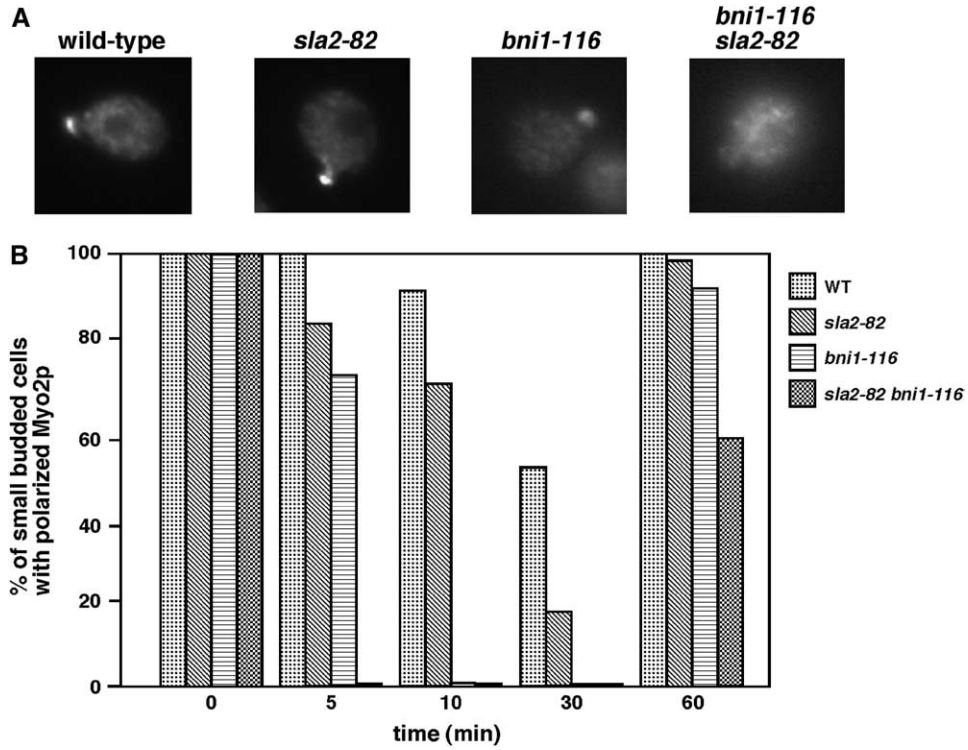

FIGURE 6.—Defects in actin-cable-dependent functions in *bni1 sla2-82* mutant cells. (A) Mislocalization of Myo2p–GFP in *bni1-116 sla2-82* mutant cells. YKT662 (*MYO2–GFP*, wild type), YKT1059 (*sla2-82 MYO2–GFP*), YKT1057 (*bni1-116 MYO2–GFP*), and YKT1061 (*bni1-116 sla2-82 MYO–GFP*) were grown in YPDA medium at 25° and then shifted to 37° for 5 min. Cells were fixed and observed by fluorescence microscopy. (B) A time course of the polarized localization of Myo2p–GFP in small-budded cells. The strains described in A were grown in YPDA medium at 25° and then shifted to 37° for the indicated periods of time. Cells were fixed and at least 200 small-budded cells were observed for each time point by fluorescence microscopy.

Sla2p binds to PtdIns(4,5)P_2 (SUN *et al.* 2005), whereas the COOH-terminal talin-like domain binds to filamentous actin (MCCANN and CRAIG 1997). In the middle of Sla2p, there are a proline-rich region, a glutamine-rich region, a leucine-zipper domain, and predicted coiled-coil regions. To obtain structural information about Sla2-82p, *sla2-82* was cloned and sequenced. *sla2-82* contained a nonsense mutation at codon 491, which resulted in the production of Sla2pΔ(491–968). In contrast to the *sla2*Δ mutant, which shows a temperature-sensitive growth phenotype (HOLTZMAN *et al.* 1993), the *sla2-82* mutant grew normally at 37°. In addition, these cells showed a slight impairment in the polarized organization of cortical actin patches and actin cables and a weakly impaired uptake of the endocytic marker Lucifer yellow (data not shown), suggesting that Sla2-82p was partially functional.

To examine the effect of the deletion of other regions of Sla2p on the growth of the Bni1pΔN-overexpressing cells, we expressed *SLA2* deletion mutants constructed previously (YANG *et al.* 1999) in cells overexpressing *BNI1*Δ*N* (Figure 9). *sla2*Δ*502-968*, which is deleted for nearly the same region with *sla2-82*, displayed the suppression. However, *sla2*Δ*768-968*, which is deleted for only the talin-like domain, did not display the suppression, suggesting that the deletion of the middle region is responsible for the suppression. Consistently, *sla2*Δ*360-575*, which is deleted for the middle region, displayed the suppression. Interestingly, *sla2*Δ*33-359*, *sla2*Δ*33-501*, and *sla2*Δ*33-750*, which are deleted for the NH_2-terminal region, did not display the suppression, irrespective of the presence or absence of the middle region, suggesting that the NH_2-terminal region is required for the suppression. Consistently, the *sla2*Δ mutant did not display the suppression (data not shown). However, NH_2-terminal deletion mutants as well as *sla2*Δ were impaired in growth at 30° (data not shown), raising a possibility that the lack of suppression was due to the impaired growth. In conclusion, our results at least suggest that deletion of the middle region of Sla2p is involved in the suppression of the growth inhibition caused by the *BNI1*Δ*N* overexpression.

DISCUSSION

***act1-301* mutant cells exhibit actin-cable-specific defects:** *act1-301* reduced the massive assembly of actin cables induced by overexpression of *BNI1*Δ*N*. Subsequent genetic studies suggested that Act1-301p inhibited formin-catalyzed actin assembly. Formin family proteins polymerize actin via a mechanism that is different from that mediated by the Arp2/3 complex. Surface amino-acid residues of actin that are important for the formin-catalyzed polymerization remain to be identified. Our isolation of *act1-301* demonstrates that these residues could be uncovered by screening cells with the mutant alleles of *ACT1* for suppressors of the *BNI1*ΔN-overexpression phenotype.

Glutamate 117, which was substituted to lysine in Act1-301p [Act1p(E117K)], is one of the Act1p surface amino-acid residues that were characterized previously by systematic charged-to-alanine mutagenesis (WERTMAN *et al.* 1992; DRUBIN *et al.* 1993). Mutations in the *act1-119*

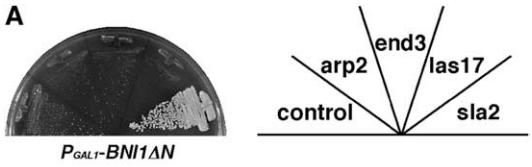

B

strain	30°C	35°C	37°C
wild-type	+++	+++	+++
bni1Δ	+++	+++	+++
sla2-82	+++	+++	+++
bni1Δ sla2-82	++	+	±
sla1Δ	+++	+++	+++
bni1Δ sla1Δ	+++	+++	+++
abp1Δ	+++	+++	+++
bni1Δ abp1Δ	+++	+++	+++
arp2-1	++	−	−
bni1Δ arp2-1	++	−	−
las17Δ	+	−	−
las17Δ bni1Δ	+	−	−

Figure 7.—A genetic interaction with *bni1* is unique to *sla2* among mutant alleles of cortical-actin-patch-related genes. (A) *arp2-1*, *end3*Δ, and *las17-11* do not suppress growth defects caused by the overexpression of *BNI1*Δ*N*. Strains grown on a YPDA plate were streaked onto a YPGA plate, followed by incubation at 30° for 2 days. The strains used were the P_{GAL1}-*BNI1*Δ*N* strain (YKT380, control) containing *arp2-2* (YKT979, arp2), *end3*Δ (YKT980, end3), *las17-11* (YKT981, las17), or *sla2-82* (YKT846, sla2). (B) Among actin-patch-related genes, only the *sla2-82* mutation shows synthetic growth defects with *bni1*Δ. Strains were streaked onto YPDA plates, followed by incubation at the indicated temperatures for 2 days. Symbols indicate the relative growth rate from wild type (+++) to no growth (−).

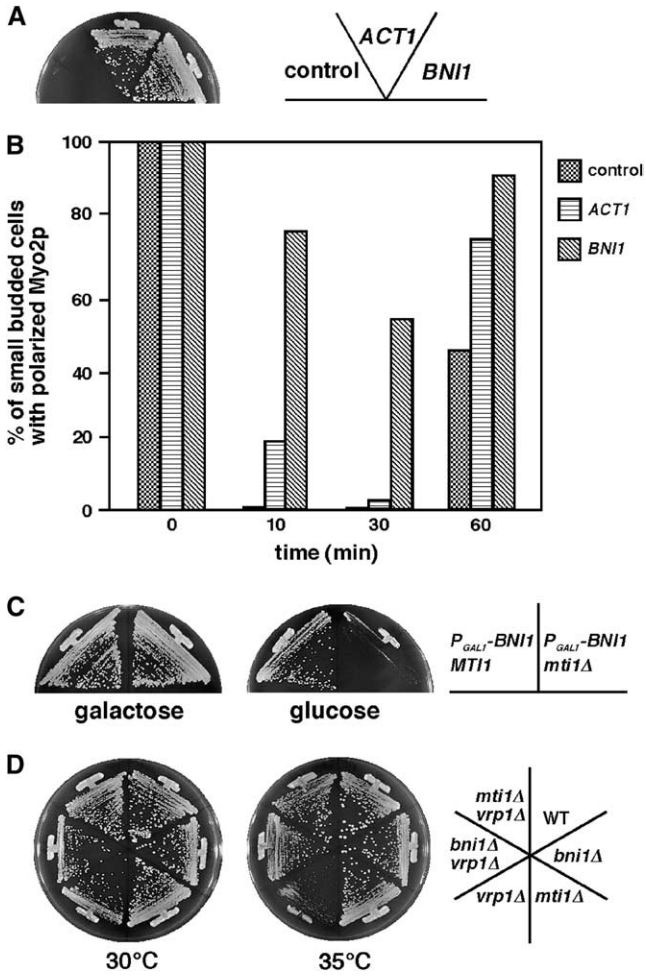

Figure 8.—Differential genetic interactions between *bni1* and regulators of actin patch assembly. (A) Suppression of the synthetic growth defects of the *bni1*Δ *sla2-82* mutant by an increased number of copies of *ACT1*. The *bni1*Δ *sla2-82* strain (YKT853) was transformed with pRS316 (control), pKT1412 (pRS316-ACT1, *ACT1*), or pKT1227 (pRS316-BNI1, *BNI1*). The transformants were streaked onto a YPDA plate, followed by incubation at 37° for 2 days. (B) Suppression of Myo2p–GFP mislocalization of the *bni1-116 sla2-82* mutant by an increased number of copies of *ACT1*. The *bni1-116 sla2-82 MYO2–GFP* strain (YKT1061) was transformed with plasmids used in A. The transformants were grown in YPDA medium at 25° and then shifted to 37° for the indicated periods of time. Cells were fixed and at least 200 small-budded cells were observed for each time point by fluorescence microscopy. (C) Synthetic growth defects of *bni1*Δ *mti1*Δ mutant cells. Strains grown on a YPGA plate were streaked onto YPGA (galactose) or YPDA (glucose) plates, followed by incubation at 37° for 2 days. P_{GAL1}-*BNI1*, YKT414; P_{GAL1}-*BNI1 mti1*Δ, YKT984. (D) Suppression of the growth defects caused by the *vrp1* mutant by *bni1* as well as *mti1*. Strains were streaked onto YPDA plates, followed by incubation at 30° or 35° for 2 days. WT, YKT38; *bni1*Δ, YKT446; *mti1*Δ, YKT189; *vrp1*Δ, YKT680; *bni1*Δ *vrp1*Δ, YKT982; *mti1*Δ *vrp1*Δ, YKT983.

allele cause three consecutive amino-acid substitutions: R116A, E117A, and K118A. However, *act1-119* did not suppress the growth defects of the Bni1pΔN-overexpressing cells (Figure 4), suggesting that the glutamate-to-lysine substitution at amino-acid position 117 may play an important role in the suppression. In contrast, the *act1-101* mutation exhibited the suppression. *act1-101(D363A, E364A)* mutant cells were found to have no actin cables at 37° (Drubin *et al.* 1993), which might be explained by weakened interactions with Pfy1p in the two-hybrid method (Amberg *et al.* 1995). Pfy1p and Bud6p bind to the FH1 and COOH-terminal domains of Bni1p, respectively, and these proteins promote actin monomers to exchange bound ADP for ATP (Moseley *et al.* 2004). In our two-hybrid experiments, Act1p(E117K) interacted normally with Pfy1p and Bud6p. *act1-301*, however, exhibited synthetic growth defects with both *pfy1-116* and *bud6*Δ, raising the possibility that Act1-p(E117K) is somewhat impaired in its ability to be acted on by Pfy1p or Bud6p. It is thought that formin FH2 dimers nucleate and processively cap the elongating barbed end of the actin filament, whereas profilin generates a local increase of ATP–actin monomers to promote actin assembly (Moseley *et al.* 2004; Romero *et al.* 2004; Otomo *et al.* 2005). The E117K and D363A

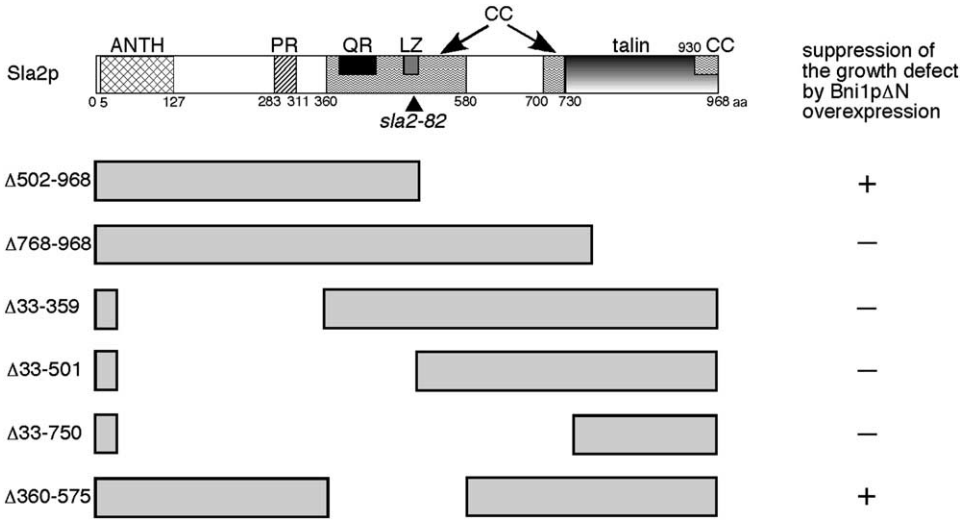

FIGURE 9.—Effect of *sla2* deletions on the growth defect caused by overexpression of a dominant active *BNI1*. C-terminal deletions were examined in YKT859 (*sla2Δ502-968*) and YKT861 (*sla2Δ768-968*), which were transformed with pRS316-P_{GAL1}-HA-BNI1ΔN. N-terminal deletions were examined in YKT1159 (*sla2Δ P_{GAL1}-HA-BNI1ΔN*), which was transformed with pRS313-sla2Δ33-359, pRS313-sla2Δ33-501, pRS313-sla2Δ33-750, or pRS313-sla2Δ360-575. The transformants were examined for growth on a galactose-containing plate (SGA–Ura or YPGA) at 30° for 3 days. The numbers indicate the positions of the amino-acid residues. The represented domains or regions are the ANTH domain (ANTH), the proline-rich region (PR), the glutamine-rich region (QR), the leucine-zipper domain (LZ), predicted coiled-coil regions (CC), and the talin-like domain (talin) (YANG *et al.* 1999; SUN *et al.* 2005). An arrowhead indicates the amino-acid residue 491 that was changed to a nonsense codon in *sla2-82*.

E364A substitutions may interfere with a step in these processes.

Genetic interactions among genes involved in the assembly of actin cables and actin patches may reflect the availability of actin monomers: The isolation of a mutation in *SLA2* as a suppressor of the *BNI1ΔN*-induced hyperaccumulation of actin cables was unexpected, because Sla2p is a regulator of cortical actin patch assembly. Synthetic growth defects of the *bni1Δ sla2-82* mutant also suggested that the *sla2-82* mutation affected the dynamics of actin cables. Given that Sla2p is involved in the negative regulation of Arp2/3-mediated actin nucleation at endocytic sites (KAKSONEN *et al.* 2003), we hypothesized that *sla2-82* interferes with actin cable assembly by depleting the available actin monomers. Consistent with this idea, increased expression of Act1p suppressed the temperature-sensitive growth phenotype of the *bni1Δ sla2-82* mutant. Suppression of *vrp1Δ* by *bni1Δ* may be similarly explained by an increased actin pool due to low levels of actin cable assembly in *bni1Δ* cells. In agreement with this hypothesis, an increased number of copies of *ACT1* suppressed the phenotype caused by *vrp1-1* (VADUVA *et al.* 1997). Although we cannot exclude the possibility that Sla2p is more directly involved in actin cable assembly, the following two observations that implicated Sla2p in polarized growth can be similarly explained by indirect effects due to actin depletion. First, *SLA2* was identified in a collection of mutants that inhibited hyperpolarized growth in *cdc34-2* mutant cells (BIDLINGMAIER and SNYDER 2002). Second, electron microscopic studies suggested that Golgi-derived secretory vesicles accumulate in *sla2* mutants (MULHOLLAND *et al.* 1997; GALL *et al.* 2002). On the basis of the observation that yeast have low levels of free actin monomers, KARPOVA *et al.* (1995) speculated that yeast actin cytoskeletons might be very static in comparison to those of motile cells wherein actin filaments can undergo very rapid cycles of assembly and disassembly. Quantitative analysis of the recovery rates of cortical actin patches after photo-bleaching, however, demonstrated that actin assembles in yeast at rates similar to those observed in motile cells (KAKSONEN *et al.* 2003). How two distinct actin-organizing systems for actin cables and actin patches can efficiently recruit and incorporate monomeric actin into actin filaments using a small pool of actin monomers remains an interesting research question.

Finally, we cannot exclude the possibility that Bni1p and Sla2p share a third function that is independent of polarized transport and endocytosis. A mutant allele of *SLA2* was identified (*mop2*; modifier of Pma1p) as an enhancer of the phenotypes caused by a mutation in *PMA1*, a gene that encodes the plasma membrane H^+-ATPase (NA *et al.* 1995). In the *mop2* mutant, the abundance of Pma1p on the plasma membrane was reduced. *SLA2* might be involved in plasma membrane integrity, because *sla2* mutations increased cell lysis as assayed by staining for extracellular alkaline phosphatase activity. Moreover, the cell-lysis phenotype was more prominent in the *bni1Δ sla2-82* mutant (data not shown). Other reports suggested that Sla2p might also be involved in mRNA and DNA metabolism. A *sla2* mutant was identified in a collection of mutants that exhibited defects in the decay of several mRNAs (ZUK *et al.* 1999). In addition, *sla1* and *sla2* mutants were found to enhance the sensitivity of cells to a self-poisoning mutant allele of DNA topoisomerase I mutant (FIORANI *et al.* 2004). It remains to be clarified whether these functions of Sla2p are mediated by the actin cytoskeleton.

We thank Rinji Akada, David Drubin, and Yoshimi Takai for yeast strains and plasmids; Eriko Itoh for technical assistance; and Konomi Kamada and members of the Tanaka Lab for helpful discussion and

advice during the course of this study. This work was supported by grants-in-aid for Scientific Research to T.Y. and K.T. from the Ministry of Education, Culture, Sports, Science, and Technology, Japan.

LITERATURE CITED

Amberg, D. C., E. Basart and D. Botstein, 1995 Defining protein interactions with yeast actin *in vivo*. Nat. Struct. Biol. **2:** 28–35.

Ayscough, K. R., J. Stryker, N. Pokala, M. Sanders, P. Crews *et al.*, 1997 High rates of actin filament turnover in budding yeast and roles for actin in establishment and maintenance of cell polarity revealed using the actin inhibitor latrunculin-A. J. Cell Biol. **137:** 399–416.

Belmont, L. D., and D. G Drubin, 1998 The yeast V159N actin mutant reveals roles for actin dynamics *in vivo*. J. Cell Biol. **142:** 1289–1299.

Bidlingmaier, S., and M. Snyder, 2002 Large-scale identification of genes important for apical growth in *Saccharomyces cerevisiae* by directed allele replacement technology (DART) screening. Funct. Integr. Genomics **1:** 345–356.

Bonnerot, C., R. Boeck and B. Lapeyre, 2000 The two proteins Pat1p (Mrt1p) and Spb8p interact *in vivo*, are required for mRNA decay, and are functionally linked to Pab1p. Mol. Cell. Biol. **20:** 5939–5946.

Carlsson, A. E., A. D. Shah, D. Elking, T. S. Karpova and J. A. Cooper, 2002 Quantitative analysis of actin patch movement in yeast. Biophys. J. **82:** 2333–2343.

Doyle, T., and D. Botstein, 1996 Movement of yeast cortical actin cytoskeleton visualized *in vivo*. Proc. Natl. Acad. Sci. USA **93:** 3886–3891.

Drubin, D. G., H. D. Jones and K. F. Wertman, 1993 Actin structure and function: roles in mitochondrial organization and morphogenesis in budding yeast and identification of the phalloidin-binding site. Mol. Biol. Cell **4:** 1277–1294.

Dunn, T. M., and D. Shortle, 1990 Null alleles of *SAC7* suppress temperature-sensitive actin mutations in *Saccharomyces cerevisiae*. Mol. Cell. Biol. **10:** 2308–2314.

Elble, R., 1992 A simple and efficient procedure for transformation of yeasts. Biotechniques **13:** 18–20.

Engqvist-Goldstein, A. E., and D. G. Drubin, 2003 Actin assembly and endocytosis: from yeast to mammals. Annu. Rev. Cell Dev. Biol. **19:** 287–332.

Evangelista, M., K. Blundell, M. S. Longtine, C. J. Chow, N. Adames *et al.*, 1997 Bni1p, a yeast formin linking Cdc42p and the actin cytoskeleton during polarized morphogenesis. Science **276:** 118–122.

Evangelista, M., D. Pruyne, D. C. Amberg, C. Boone and A. Bretscher, 2002 Formins direct Arp2/3-independent actin filament assembly to polarize cell growth in yeast. Nat. Cell Biol. **4:** 32–41.

Evangelista, M., S. Zigmond and C. Boone, 2003 Formins: signaling effectors for assembly and polarization of actin filaments. J. Cell Sci. **116:** 2603–2611.

Fiorani, P., R. J. Reid, A. Schepis, H. R. Jacquiau, H. Guo *et al.*, 2004 The deubiquitinating enzyme Doa4p protects cells from DNA topoisomerase I poisons. J. Biol. Chem. **279:** 21271–21281.

Gall, W. E., N. C. Geething, Z. Hua, M. F. Ingram, K. Liu *et al.*, 2002 Drs2p-dependent formation of exocytic clathrin-coated vesicles *in vivo*. Curr. Biol. **12:** 1623–1627.

Gietz, R. D., and R. A. Woods, 2002 Transformation of yeast by lithium acetate/single-stranded carrier DNA/polyethylene glycol method. Methods Enzymol. **350:** 87–96.

Govindan, B., R. Bowser and P. Novick, 1995 The role of Myo2, a yeast class V myosin, in vesicular transport. J. Cell Biol. **128:** 1055–1068.

Hollenberg, S. M., R. Sternglanz, P. F. Cheng and H. Weintraub, 1995 Identification of a new family of tissue-specific basic helix-loop-helix proteins with a two-hybrid system. Mol. Cell. Biol. **15:** 3813–3822.

Holtzman, D. A., S. Yang and D. G. Drubin, 1993 Synthetic-lethal interactions identify two novel genes, *SLA1* and *SLA2*, that control membrane cytoskeleton assembly in *Saccharomyces cerevisiae*. J. Cell Biol. **122:** 635–644.

Imamura, H., K. Tanaka, T. Hihara, M. Umikawa, T. Kamei *et al.*, 1997 Bni1p and Bnr1p: downstream targets of the Rho family small G-proteins which interact with profilin and regulate actin cytoskeleton in *Saccharomyces cerevisiae*. EMBO J. **16:** 2745–2755.

Kadota, J., T. Yamamoto, S. Yoshiuchi, E. Bi and K. Tanaka, 2004 Septin ring assembly requires concerted action of polarisome components, a PAK kinase Cla4p, and the actin cytoskeleton in *Saccharomyces cerevisiae*. Mol. Biol. Cell **15:** 5329–5345.

Kaksonen, M., Y. Sun and D. G. Drubin, 2003 A pathway for association of receptors, adaptors, and actin during endocytic internalization. Cell **115:** 475–487.

Kamei, T., K. Tanaka, T. Hihara, M. Umikawa, H. Imamura *et al.*, 1998 Interaction of Bnr1p with a novel Src homology 3 domain-containing Hof1p. Implication in cytokinesis in *Saccharomyces cerevisiae*. J. Biol. Chem. **273:** 28341–28345.

Karpova, T. S., K. Tatchell and J. A. Cooper, 1995 Actin filaments in yeast are unstable in the absence of capping protein or fimbrin. J. Cell Biol. **131:** 1483–1493.

Karpova, T. S., S. L. Reck-Peterson, N. B. Elkind, M. S. Mooseker, P. J. Novick *et al.*, 2000 Role of actin and Myo2p in polarized secretion and growth of *Saccharomyces cerevisiae*. Mol. Biol. Cell **11:** 1727–1737.

Kawahata, M., S. Amari, Y. Nishizawa and R. Akada, 1999 A positive selection for plasmid loss in *Saccharomyces cerevisiae* using galactose-inducible growth inhibitory sequences. Yeast **15:** 1–10.

Kikyo, M., K. Tanaka, T. Kamei, K. Ozaki, T. Fujiwara *et al.*, 1999 An FH domain-containing Bnr1p is a multifunctional protein interacting with a variety of cytoskeletal proteins in *Saccharomyces cerevisiae*. Oncogene **18:** 7046–7054.

Longtine, M. S., A. McKenzie, III, D. J. Demarini, N. G. Shah, A. Wach *et al.*, 1998 Additional modules for versatile and economical PCR-based gene deletion and modification in *Saccharomyces cerevisiae*. Yeast **14:** 953–961.

McCann, R. O., and S. W. Craig, 1997 The I/LWEQ module: a conserved sequence that signifies F-actin binding in functionally diverse proteins from yeast to mammals. Proc. Natl. Acad. Sci. USA **94:** 5679–5684.

Mochida, J., T. Yamamoto, K. Fujimura-Kamada and K. Tanaka, 2002 The novel adaptor protein, Mti1p, and Vrp1p, a homolog of Wiskott-Aldrich syndrome protein-interacting protein (WIP), may antagonistically regulate type I myosins in *Saccharomyces cerevisiae*. Genetics **160:** 923–934.

Moseley, J. B., I. Sagot, A. L. Manning, Y. Xu, M. J. Eck *et al.*, 2004 A conserved mechanism for Bni1- and mDia1-induced actin assembly and dual regulation of Bni1 by Bud6 and profilin. Mol. Biol. Cell **15:** 896–907.

Mulholland, J., D. Preuss, A. Moon, A. Wong, D. Drubin *et al.*, 1994 Ultrastructure of the yeast actin cytoskeleton and its association with the plasma membrane. J. Cell Biol. **125:** 381–391.

Mulholland, J., A. Wesp, H. Riezman and D. Botstein, 1997 Yeast actin cytoskeleton mutants accumulate a new class of Golgi-derived secretary vesicle. Mol. Biol. Cell **8:** 1481–1499.

Na, S., M. Hincapie, J. H. McCusker and J. E. Haber, 1995 *MOP2* (*SLA2*) affects the abundance of the plasma membrane H(+)-ATPase of *Saccharomyces cerevisiae*. J. Biol. Chem. **270:** 6815–6823.

Otomo, T., D. R. Tomchick, C. Otomo, S. C. Panchal, M. Machius *et al.*, 2005 Structural basis of actin filament nucleation and processive capping by a formin homology 2 domain. Nature **433:** 488–494.

Ozaki, K., K. Tanaka, H. Imamura, T. Hihara, T. Kameyama *et al.*, 1996 Rom1p and Rom2p are GDP/GTP exchange proteins (GEPs) for the Rho1p small GTP binding protein in *Saccharomyces cerevisiae*. EMBO J. **15:** 2196–2207.

Pring, M., M. Evangelista, C. Boone, C. Yang and S. H. Zigmond, 2003 Mechanism of formin-induced nucleation of actin filaments. Biochemistry **42:** 486–496.

Pruyne, D., and A. Bretscher, 2000 Polarization of cell growth in yeast. II. The role of the cortical actin cytoskeleton. J. Cell Sci. **113:** 571–585.

Pruyne, D. W., D. H. Schott and A. Bretscher, 1998 Tropomyosin-containing actin cables direct the Myo2p-dependent polarized delivery of secretory vesicles in budding yeast. J. Cell Biol. **143:** 1931–1945.

Pruyne, D., M. Evangelista, C. Yang, E. Bi, S. Zigmond *et al.*, 2002 Role of formins in actin assembly: nucleation and barbed-end association. Science **297:** 612–615.

Raths, S., J. Rohrer, F. Crausaz and H. Riezman, 1993 *end3* and *end4*: two mutants defective in receptor-mediated and fluid-phase endocytosis in *Saccharomyces cerevisiae*. J. Cell Biol. **120:** 55–65.

Rodal, A. A., A. L. Manning, B. L. Goode and D. G. Drubin, 2003 Negative regulation of yeast WASp by two SH3 domain-containing proteins. Curr. Biol. **13:** 1000–1008.

Romero, S., C. Le Clainche, D. Didry, C. Egile, D. Pantaloni *et al.*, 2004 Formin is a processive motor that requires profilin to accelerate actin assembly and associated ATP hydrolysis. Cell **119:** 419–429.

Sagot, I., S. K. Klee and D. Pellman, 2002a Yeast formins regulate cell polarity by controlling the assembly of actin cables. Nat. Cell Biol. **4:** 42–50.

Sagot, I., A. A. Rodal, J. Moseley, B. L. Goode and D. Pellman, 2002b An actin nucleation mechanism mediated by Bni1 and profilin. Nat. Cell Biol. **4:** 626–631.

Sherman, F., 2002 Getting started with yeast. Methods Enzymol. **350:** 3–41.

Sheu, Y. J., B. Santos, N. Fortin, C. Costigan and M. Snyder, 1998 Spa2p interacts with cell polarity proteins and signaling components involved in yeast cell morphogenesis. Mol. Cell. Biol. **18:** 4053–4069.

Sheu, Y. J., Y. Barral and M. Snyder, 2000 Polarized growth controls cell shape and bipolar bud site selection in *Saccharomyces cerevisiae*. Mol. Cell. Biol. **20:** 5235–5247.

Shortle, D., P. Novick and D. Botstein, 1984 Construction and genetic characterization of temperature-sensitive mutant alleles of the yeast actin gene. Proc. Natl. Acad. Sci. USA **81:** 4889–4893.

Sikorski, R. S., and P. Hieter, 1989 A system of shuttle vectors and yeast host strains designed for efficient manipulation of DNA in *Saccharomyces cerevisiae*. Genetics **122:** 19–27.

Smith, M. G., S. R. Swamy and L. A. Pon, 2001 The life cycle of actin patches in mating yeast. J. Cell Sci. **114:** 1505–1513.

Sun, Y., M. Kaksonen, D. T. Madden, R. Schekman and D. G. Drubin, 2005 Interaction of Sla2p's ANTH domain with PtdIns(4,5)P_2 is important for actin-dependent endocytic internalization. Mol. Biol. Cell **16:** 717–730.

Tong, A. H., M. Evangelista, A. B. Parsons, H. Xu, G. D. Bader *et al.*, 2001 Systematic genetic analysis with ordered arrays of yeast deletion mutants. Science **294:** 2364–2368.

Vaduva, G., N. C. Martin and A. K. Hopper, 1997 Actin-binding verprolin is a polarity development protein required for the morphogenesis and function of the yeast actin cytoskeleton. J. Cell Biol. **139:** 1821–1833.

Vojtek, A. B., S. M. Hollenberg and J. A. Cooper, 1993 Mammalian Ras interacts directly with the serine/threonine kinase Raf. Cell **74:** 205–214.

Waddle, J. A., T. S. Karpova, R. H. Waterston and J. A. Cooper, 1996 Movement of cortical actin patches in yeast. J. Cell Biol. **132:** 861–870.

Wertman, K. F., D. G. Drubin and D. Botstein, 1992 Systematic mutational analysis of the yeast *ACT1* gene. Genetics **132:** 337–350.

Yang, S., M. J. Cope and D. G. Drubin, 1999 Sla2p is associated with the yeast cortical actin cytoskeleton via redundant localization signals. Mol. Biol. Cell **10:** 2265–2283.

Zuk, D., J. P. Belk and A. Jacobson, 1999 Temperature-sensitive mutations in the *Saccharomyces cerevisiae MRT4*, *GRC5*, *SLA2* and *THS1* genes result in defects in mRNA turnover. Genetics **153:** 35–47.

Communicating editor: T. Stearns